MEASUREMENT-BASED 60 GHZ TAPPED-DELAY-LINE CHANNEL MODEL

Radek Zavorka
Doctoral Degree Programme (1), FEEC BUT
E-mail: xzavor03@stud.feec.vutbr.cz

Supervised by: Ales Prokes
E-mail: prokes@feec.vutbr.cz

Abstract: With the development of communication technology a new electromagnetic spectrum is necessary. It is the reason for the research of millimeter waves (MMW) about 60 GHz. This paper is focused on the evaluation impact of multipath components on receive signals. It depends on the radiation pattern of used antennas and the direction of the receiving antenna related to the line of sight (LOS) component. The multipath components (MPCs) are received from surrounding points around the center of the transmitter. To model the MPCs propagation a basic Tap Delay Line (TDL) model is established including individual tap indexes and important points are compared mutually. Research is also focused on the determination of the reflectivity of the surrounding objects.

Keywords: channel measurement, mmWave, Power Delay Profile, Tapped Delay Line

1 INTRODUCTION

Millimeter waves are defined as the electromagnetic spectrum from 30 to 300 GHz. Due to the growing requirements on communication speed, it was a logical step to move to the higher frequency. Band of mmWave offers a wide range of possibilities, like a wider communication spectrum and a higher frequency, which allow the rise of the communication speed. Another reason was the abrupt increase of the number of communication devices, because they need individual bands for transmitting signals. There are a few unlicensed industrial, scientific, and medical (ISM) frequency bands specially designated for high speed, indoor and outdoor connectivity.

The 60 GHz mmWave is a perspective ISM band and the International Telecommunication Union (ITU) suggested it for unlicensed operation. Many researchers study the propagation of this wave for various environments and applications. The physical limitations are predominantly caused by the extremely high propagation path loss reducing the propagation range, since the path loss increases with the square of frequency. A potential problem for longer propagation distances can also be caused by rain attenuation and absorption of MMW energy by the resonance of oxygen and water vapor molecules in the atmosphere. Heavy rain can cause attenuation of about 12 dB/km at 60 GHz, while attenuation about 15 dB/km is excited by oxygen in the frequency band 57-64 GHz. Modern equipment and laboratories are necessary for the demonstrative approach because common measuring devices aren't sufficient. The paper [1] presents results obtained from a vehicle-to-vehicle channel measurement campaign carried out in the millimeter-wave band around a 60 GHz. In [2] you can see the study of propagation mmWave inside a bus. In the article [3] authors measured and modeled mmWave channel for outdoor microcellular environment and a very large waiting hall at a railway station at 26 and 28 GHz.

2 MEASUREMENT SCENARIO

The measurement simulates a static vehicle to infrastructure communication. It was performed in the Brno University of Technology campus between the building at Technicka 12 and VW CC car park on the far side of the road as shown in Fig. 1a. A transmit omnidirectional antenna together with the power amplifier and cooler were placed on the roof of the car. And a receiver with a horn antenna was situated in a window on the 6th floor of the university building. Receiving antenna scanned the area around the car and measured multipath components (MPCs), see points in Fig. 1b. A motorized Sky-Watcher AllView mount controlled by PC and LabView was used to direct the antenna. From Fig. 1a it is obvious that the height of the transmitting (TX) and receiving (RX) antennas above the ground is h = 1.55 m and H = 14.5 m respectively. Because the distance between the TX antenna and the building is D = 28.5 m, the propagation distance between the antennas is $L = \sqrt{(H-h)^2 + D^2} = 31.3$ m.

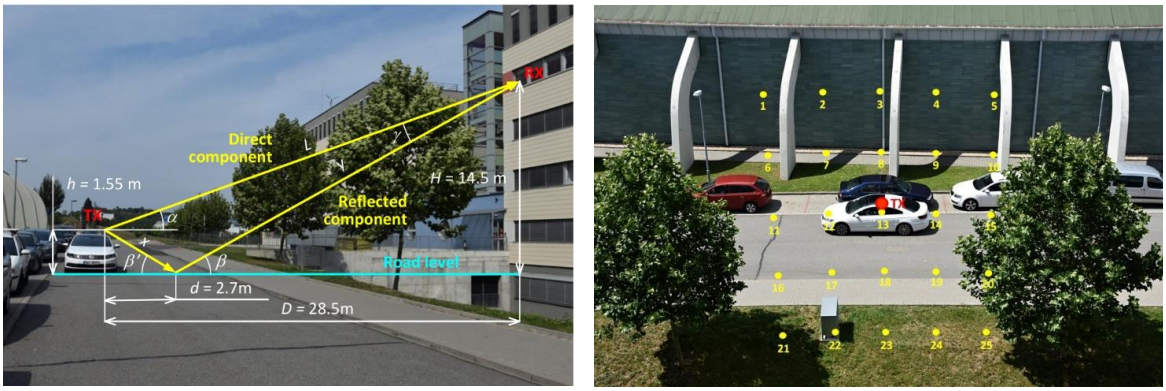

a) b)

Figure 1: Position of the transmitter relative to the receiver a), measurement points b). [4]

3 MEASUREMENT SETUP

The channel measurement was carried out using the 60 GHz time-domain channel sounder described in detail in [4]. The transmitter is based on an Anritsu MP1800A Signal Quality Analyzer working as a pseudorandom binary sequence (PRBS) generator. The receiver is created using a Tektronix MSO72004C (20 GHz, 50 GS/s) Mixed Signal Oscilloscope working as a very fast analog-to-digital converter. The baseband PRBS signal is converted into the MMW band and back using SiversIma FC1000V series V-band up/down converters [5]. The channel sounder bandwidth is 8 GHz, the number of samples per measured channel impulse response (CIR) is set to N_{Sa} = 8092 and the number of saved CIRs per measurement is N_{CIR} = 932. Due to the correlation gain and averaging, the sounder dynamic range is about 55 dB. The transmitter was equipped with an omnidirectional SIW slot antenna described in [6], whose radiation pattern related to the car is shown in Fig. 2. The MMW signal was received using a directional horn antenna with a dielectric lens. The antenna gain depends on the angle which is shown in Fig. 3. All measured values mentioned below are related to the low noise MMW preamplifier output. After that, the down converter SiversIma increases them by a gain of about 15-20 dB.

4 CHANNEL CHARACTERIZATION

In this work, the static channel is analyzed which means that the position of all objects is stable in time. The channel is often modeled by the linear time invariant filter (LTI), where the impulse

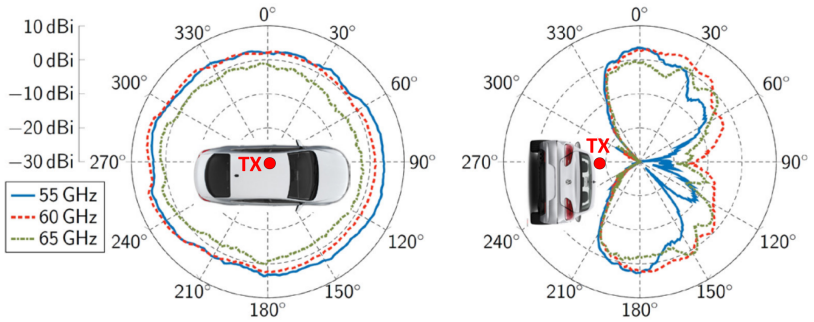

Figure 2: E-plane (left) and H-plane (right) measured radiation pattern of double-sided SIW slot antenna at 55 GHz, 60 GHz, and 65 GHz. [4]

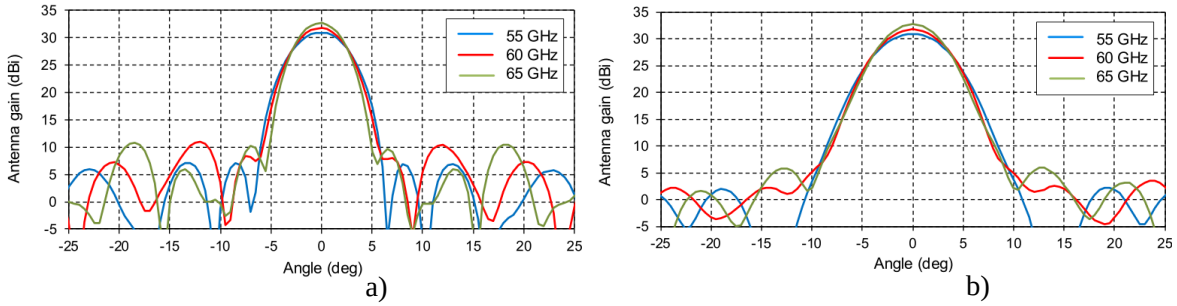

a) b)

Figure 3: E-plane a) and H-plane b) measured gain of horn antenna. [4]

response of the channel is marked $h(t)$, and the output is presented as a convolution of a useful signal with an impulse response and then noise $n(t)$ is added.

$$r(t) = s(t) * h(t) + n(t) \tag{1}$$

The main focus is to analyze a power delay profile (PDP) for the line of sight and nonLOS (NLOS) components. Special attention will be paid to the evaluation of the influence of the surrounding objects to the power received from different directions. Fig. 4 shows the received power from all points.

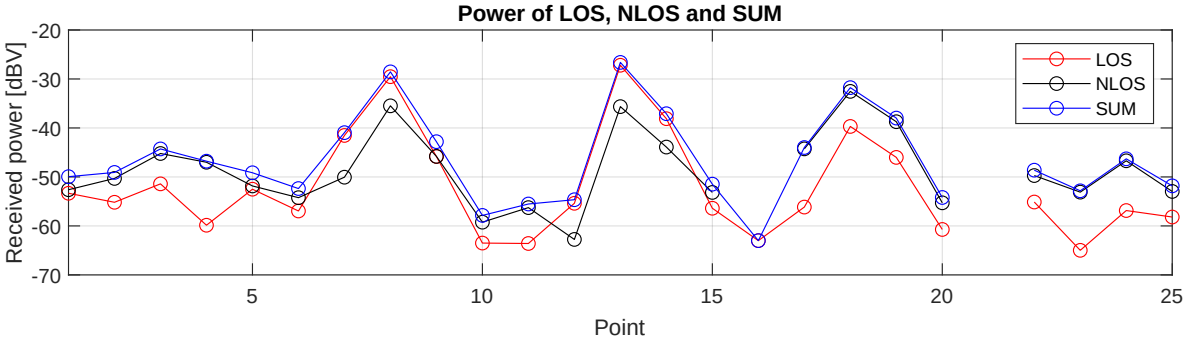

Figure 4: Power of received signal.

The red line means LOS power, black line is the sum of individual components of the channel impulse responses (CIRs) for NLOS and the blue line is the total received power from each point. It is evident that the strongest component is received from the direct path (point 13). Also the nearest points have relatively strong components in LOS and NLOS, but most significantly it is in a vertical direction from the centre for points 8, 18 and also 7, 9, 14, 17, 19. It is due to the radiation pattern of both antennas, Fig. 2 and 3.

From this measurement it is also possible to estimate the reflectivity of individual objects or surfaces. As is evident from the graph in Fig. 4 a satisfactory reflection off the surface of the road or sidewalk was achieved. It can be caused by very smooth sections of the road, because the length of waves is extremely short, about 5 millimeters. There is a very good reflectivity of the building behind the car. NLOS components have a higher intensity, about 6-12 dB, than their LOS. On the other hand, the grass surface and clay exhibit higher losses, it is about 30 dB in comparison with the direct path from the center point 13. Of course, branches and leaves of a tree cause a significant attenuation of the signal due to the fading effect. A metal box (point 22 in Fig. 1b) doesn't cause such important losses in the MPCs. This might be caused by the ray refraction on the edge.

4.1 TDL MODEL

Tapped delay line model for every point from Fig. 1b is analyzed from the performed measurement. This model corresponds to the Finite Impulse Response (FIR) filter and the general model is shown in Fig. 5. Equation (2) describes the output of TDL and corresponds with the general model:

$$y(\tau) = \sum_{n=1}^{N} s(\tau - nT) g_n(\tau), \tag{2}$$

where $s(\tau)$ is a delay input signal and $g_n(\tau)$ are TDL tap gains. Every tap index is obtained from a 10 ns cluster like max value, which allows to distinguish 3 meters differences in the length of the signal path. The reason why the clusters are established is to create a simplified model. To evaluate normalized tap gain, the max value of CIRs is taken from the cluster, because there are sometimes very weak components, which isn't significant.

In Fig. 6, there are important points from Fig. 1b where normalized tap gains are shown in the bar chart depending on the delay and normalized in the view of LOS. The value of LOS is in the title of the graph. Strength of the received power depends on the angle of the rotation of the receiving antenna and reflectivity surface, as described above. Differences between propagation path lengths of NLOS components are described above the dominant components.

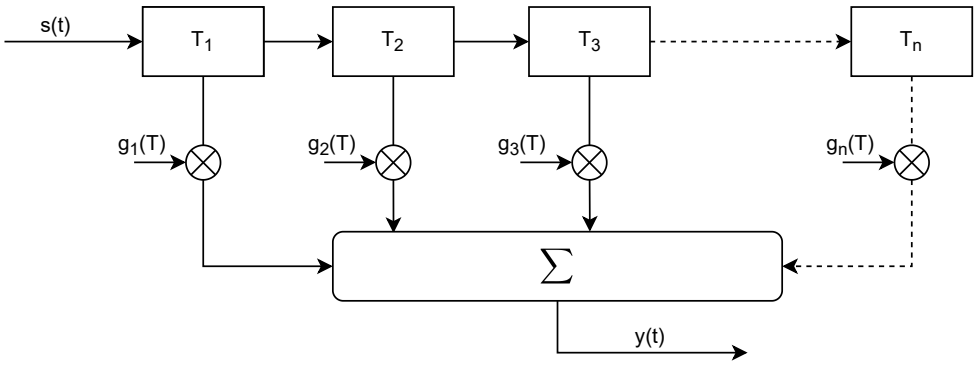

Figure 5: General model of Tapped Delay Line.

When a signal is received from a direct path from point 13, there is only one tap index whose value considerably exceeds other components, but it is significantly attenuated in comparison with LOS. It is due to the radiation pattern of the receiving antenna, because the incoming signal that is skewed five degrees from the direct path is significantly attenuated. Point 8 has an important index 4, which shows a reflected signal with a longer way, about 12 m. It corresponds with the distance between the car and the sidewalk near the building behind the car. Other components for this point are much less

significant. Points 17, 18, 19 are interesting due to the first tap index, which contains a reflected signal with a distance of about 3 m from the LOS. It is the same case as point 13, the antenna is heading to the road and the edge of the lobe is receiving a signal from the center point. It is obvious that the surface of the road has a very good reflectivity. TDL models for these three points have another tap index with a delay between 80-90 ns, which corresponds with the difference of the distances of about 24-27 m. The component at the tap 8/9 is strongly attenuated due to the large path loss and also due to the multi-reflection. The signal is probably reflected from the building behind the car and from the surrounding car body, whose surface reflects the signal very well.

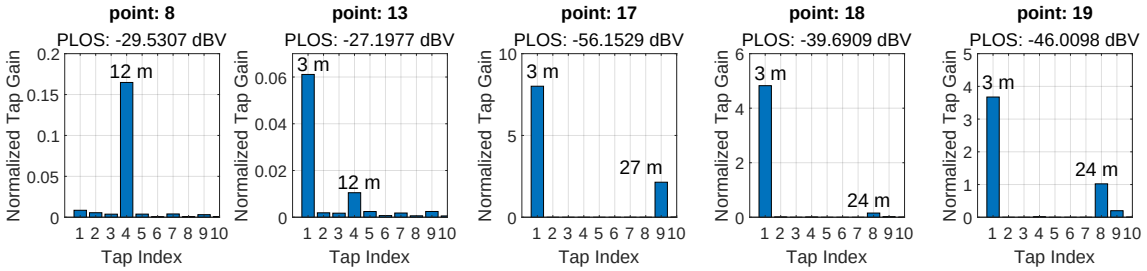

Figure 6: Normalized tap gain for select points.

5 CONCLUSION

This paper offers general information about the mmWave propagation and provides instructions for channel measurement. The main goal of this work is to analyze the multipath components between the transmitter located on the roof of the car and the receiver situated in the window of the building. It is found that the strongest power was received from the direct path and from the nearest points around the transmitter. MPCs have a significant influence when they are reflected from the road and sidewalk because the delayed received signal has a considerably greater amplitude than LOS (for a given antenna direction). Also, it is found that the grass surface attenuated the signal very well (more than 30 dB in relation to the center point). TDL model is defined for every point and the most significant components are described and shown with the value of delay time and distance.

REFERENCES

[1] J. Blumenstein et al., *Vehicle-to-Vehicle Millimeter-Wave Channel Measurements at 56-64 GHz*, IEEE 90th VTC, Honolulu, HI, USA, 2019, pp. 1-5.

[2] A. Chandra et al., *60 GHz millimeter wave propagation inside bus: Measurement, modeling, simulation, and performance analysis*, IEEE Access, vol. 7, no. 2019, pp. 97815-97826.

[3] X. Zhao et al., *Neural network and GBSM based time-varying and stochastic channel modeling for 5G millimeter wave communications*, in China Communications, vol. 16, no. 6, pp. 80-90, June 2019, doi: 10.23919/JCC.2019.06.007.

[4] A. Prokes et al., *Multipath Propagation Analysis for Vehicle-to-Infrastructure Communication at 60 GHz*, 2019 IEEE Vehicular Networking Conference (VNC), Los Angeles, CA, USA, 2019, pp. 1-8, doi: 10.1109/VNC48660.2019.9062771.

[5] *FC1005V/00 V-band Converter with LO*. [Online]. [Accessed: 16-Feb-2021]. Available: https://www.ecmstockroom.com/writable/items/pdf_files/fc1005v00-data-sheet.pdf

[6] T. Mikulasek, J. Lacik, and Z. Raida, *SIW slot antennas utilized for 60- GHz channel characterization*, Microw Opt. Tech. Lett., vol. 57, no. 6, pp. 1365-1370, 2015.